Modeling and Evaluating Systematic and Random Errors in Multiscale GPM IMERG Summer Precipitation Estimates Over the Sichuan Basin

Shunxian Tang, Rui Li, and Jianxin He

***Abstract*—The Integrated Multi-satellitE Retrievals for the Global Precipitation Measurement (IMERG) is widely used in hydrological and meteorological studies, owing to its high spatial resolution and accuracy. The quantification of systematic and random errors for the IMERG estimates at different temporal resolutions is beneficial to the calibration of observation instruments and correction of estimates, especially for regions such as the Sichuan Basin where frequent geological disasters occur in the summer. At present, there are two most commonly used models, namely the additive and multiplicative models, for modeling the systematic and random errors of precipitation. However, it is unknown which model is more suitable for the IMERG summer hourly, daily, and monthly precipitation estimates. Therefore, in this study, two models' separative capability of the systematic and random errors and predictive capability in the IMERG estimates are investigated, upon the evaluation of the models' applicability. Results show that for the hourly and daily precipitation estimates, the multiplicative error model has better separative and predictive capabilities than the additive error model and is recommended to quantify the systematic and random errors. Conversely, as for the monthly precipitation estimates, the additive error model is a relatively better choice by comparing the overall performance of both models. However, it still has some weaknesses for heavy monthly precipitation, such as nonconstant fluctuations and reduced predictive capability. So, the additive model should be used with caution in analyzing the systematic and random errors of the heavy monthly precipitation.**

***Index Terms*—Error model, Integrated Multi-satellitE Retrievals for GPM (IMERG), summer precipitation, systematic and random errors.**

I. Introduction

PRECIPITATION is one of the most important components of the global water cycle and energy exchange at the Earth's surface [1], [2]. Accurate measurements of precipitation are very important not only for weather forecasting and climate research, but also for the early warning of rainfall-induced geological disasters, management of agricultural water resources, and formulation of urban drought and flood risk application strategies [3]–[5].

Compared to conventional quantitative precipitation observation technologies such as rain gauges and ground-based weather radars, satellite-based remote sensing may be the most reliable and stable way to obtain precipitation information on a global scale [5]–[7]. Since the advent of meteorological satellites in the 1970s, the techniques of obtaining global precipitation by satellite have advanced rapidly. Specifically, satellite remote-sensing techniques have evolved from the original visible and infrared remote sensing to passive microwave sensors, and then to the present active microwave sensors. Meanwhile, the accuracy of satellite-based precipitation estimates keeps improving.

Since the successful launch of the Tropical Rainfall Measuring Mission (TRMM) carrying the first Ku-band active Precipitation Radar (PR) in 1997, the satellite-based precipitation estimates play an increasingly important role in the observation of global precipitation. As a successor to the TRMM, the Global Precipitation Measurement (GPM) mission satellite, which equipped with a dual-frequency precipitation radar (Ku-band and Ka-band, DPR), was launched in 2014. GPM has a wider monitoring region than TRMM [5]. Both TRMM and GPM provide multisatellite estimates, namely the TRMM Multi-satellite Precipitation Analysis (TMPA) [8] and the Integrated Multi-satellitE Retrievals for GPM (IMERG) [9], and their highest spatiotemporal resolutions are $0.25^\circ \times 3$ h and $0.1^\circ \times 0.5$ h, respectively. At present, previous studies have found that the IMERG estimates outperform TMPA standard estimates, suggesting better capturing capability and higher estimation accuracy of precipitation [7], [10]–[15]. Therefore, the GPM IMERG estimates with high spatiotemporal resolution and measurement accuracy are one of the most widely used products in the field of atmospheric science and hydrological remote sensing [16]–[19].

However, in the process of the IMERG estimates generation, such as data collection, data integration, and precipitation retrieval, errors are inevitable, which are more obvious for summer precipitation [20], [21] due to its large dynamic range. More generally, the uncertainties of the precipitation estimate mainly include the systematic errors and random errors. Quantifying the uncertainties of the IMERG estimates will benefit many scientific studies, such as discussing climate change, revealing

Manuscript received February 1, 2021; revised March 28, 2021 and April 20, 2021; accepted April 24, 2021. Date of publication April 28, 2021; date of current version May 24, 2021. This work was supported in part by the National Key R&D Program of China under Grant 2018YFC1506100 and Grant 2018YFC1506101, and in part by the Natural Science General Project of Sichuan Education Department under Grant 18ZB0113. *(Corresponding authors: Rui Li; Jianxin He.)*

Shunxian Tang and Rui Li are with the College of Meteorological Observation, Chengdu University of Information Technology, Chengdu 610225, China (e-mail: tsx@cuit.edu.cn; lirui87@cuit.edu.cn).

Jianxin He is with the Key Laboratory of Atmospheric Sounding, China Meteorological Administration, Chengdu 610225, China (e-mail: hjx@cuit.edu.cn).

Digital Object Identifier 10.1109/JSTARS.2021.3076197

the influence mechanism of the hydrological cycle, improving the quality of input data for numerical prediction models, as well as accurately calibrating spaceborne instruments.

Some studies have conducted mathematical models for error analysis of the satellite-based precipitation products [22]–[27]. However, most of these models involve complex computational processes. Giving the models simple and easy to implement, we attempt to select a mathematical model, whether implicitly or explicitly, that can accurately describe the error characteristics in the IMERG precipitation estimates. Although the source and influence mechanism of errors do not directly determine the choice of error models, an excellent error model is an accurate mathematical description of a measurement's deviation from the truth [28]. The additive and multiplicative models are the two most commonly used error models for precipitation measurements. The quantitative analysis and statistical examination on the errors of the precipitation estimates with selected prototype models will help the model parameters calculation and improvement. If there are just ground references or satellite precipitation estimates available, the specific error model can be used to predict measurements and their errors, thus achieving "inverse calibration."

Regarding the selection of precipitation error model, many researches have adopted the additive model in evaluating the error characteristics of various precipitation products, including the Precipitation Estimation from Remotely Sensed Information using Artificial Neural Networks (PERSIANN) [29], the CPC MORPHing (CMORPH) [30], the Global Satellite Mapping of Precipitation (GSMaP) [31], TMPA [8], the Estimation of Precipitation by Satellites-Second Generation (EPSAT-SG) [6], [32]–[36]. However, some other researches have used the multiplicative error model to quantify or simulate the errors in precipitation estimates such as WSR-88D radar rainfall estimates, TMPA, and IMERG [37]–[40].

Because different error models represent completely different error definitions, for a specific precipitation product, we can choose a more reasonable error model only after comparing and analyzing the applicability of several error models. Tian *et al*. [27] assessed the suitability of the multiplicative and additive error models for the TMPA real-time daily precipitation estimates over the Oklahoma region and proposed that the multiplicative error model is a better choice. Alemohammad *et al*. [41] introduced the multiplicative model in the Triple Collocation method for biweekly precipitation error analysis and found that the multiplicative model is more realistic than the additive error model used in the Triple Collocation derivations. Tang *et al*. [42] discussed on the systematic and random errors of four daily satellite precipitation products including IMERG using the additive and multiplicative models in China and suggested that the multiplicative model is superior to the additive model. It should be noted that the temporal resolution of the precipitation products used in the above studies is daily or biweekly. However, the IMERG precipitation estimates with higher and coarser temporal resolutions are widely used in many applications, provided that the errors of these products can be described quantitatively. This raises the question of whether their conclusions are still robust and reliable for satellite precipitation products with other temporal resolutions (e.g., hourly and monthly). Our previous study has shown that the errors of the IMERG summer precipitation mainly come from the hit precipitation and are much larger than those of other seasonal precipitation over the Sichuan Basin of China [21]. In addition, this area is prone to geological disasters caused by summer heavy rain [43]. Regrettably, little research focused on the quantification or modeling of the errors for the IMERG summer precipitation in this area. Therefore, it is worth studying which error model is more suitable for the hourly, daily, and monthly GPM IMERG summer precipitation estimates over the Sichuan Basin. Research on this issue will help data producers and users to more clearly understand the uncertainties of the precipitation estimates and thus promote the improvement and application of products. To achieve this goal, we refer to the criteria proposed by Tian *et al*. [27] and evaluate the suitability of the two models: 1) Can the model effectively separate the systematic and random errors? (i.e., model's separative capability) and 2) Can the model accurately reproduce future precipitation characteristics? (i.e., model's predictive capability).

The remaining sections of the article are structured as follows: The study area, GPM IMERG precipitation estimates, and ground reference data are introduced in Section II. The principles of two error models and data preprocessing methods are described in Section III. Section IV presents the performance comparison results of the two error models for the hourly, daily, and monthly IMERG precipitation estimates. Finally, the discussion and conclusion are provided in Sections V and VI.

II. Study Area and Datasets

A. Study Area

Sichuan Basin (28°15′-32°03′N, 103°03′-109°15′E), located in the central part of western China, is the most typical basin with the lowest altitude among the four major basins in China. As the transition area from the plateau topography (Yunnan-Guizhou Plateau, Qinghai-Tibet Plateau) to the eastern plain of China, Sichuan Basin covers the central and eastern parts of Sichuan province and most of Chongqing city, with a total area of about 2.6×10^5 km^2. In addition, Sichuan Basin can be clearly divided into the marginal mountains (1.0×10^5 km^2) and basin floors (1.6×10^5 km^2). The marginal mountains are mostly surrounded by mountains with elevations between 1000 and 3000 m, while the elevations of the basin floors are between 250 and 750 m, and the contour of the entire basin is approximately diamond shaped. The unique geographical location has a great influence on the spatial distribution and intensity of precipitation in the basin, especially for summer precipitation [43]–[45]. Specifically, heavy precipitation in summer has the characteristics of frequent occurrence, strong localization, and a wide range of intensity change, which is obviously different from the eastern region of the same latitude [46], [47]. Thus, geological disasters caused by summer heavy precipitation, such as collapse-landslide, ground subsidence, and debris flow often occur.

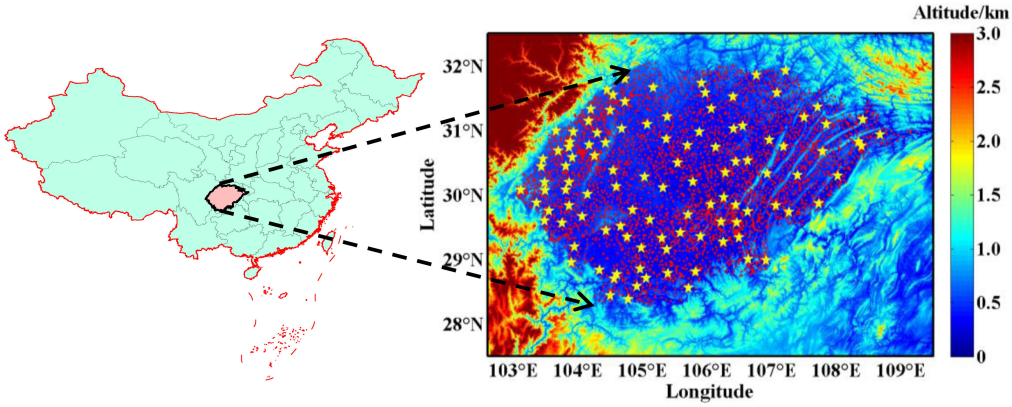

Fig. 1. Geographical location, digital elevation model (DEM), and gauge stations of the study area: the small red dot and the big yellow pentagram represent regional and national gauge station, respectively.

B. GPM IMERG Precipitation Estimates

GPM mission is jointly developed by the National Aeronautics Space Administration (NASA) and the Japan Aerospace Exploration Agency (JAXA), including one core observatory and approximately ten constellation satellites [5]. The GPM core observatory carries two primary sensors: a 13-channel passive microwave imager and a dual-frequency precipitation radar, which are used to detect the internal structure of precipitation and improve the ability to capture light-intensity precipitation (< 0.5 mm/h) and solid precipitation [48]. IMERG is one of the most important GPM precipitation estimates and provides the "Early Run" (IMERG-E), "Late Run" (IMERG-L), and "Final Run" (IMERG-F) products at relatively fine spatiotemporal resolution ($0.1^\circ \times 0.5$ h). The IMERG-F is supposed to be a better product in terms of precipitation estimation accuracy. More details about the three IMERG precipitation estimates and retrieval algorithms are available in Huffman *et al.* [9].

Note that the choice of error model depends on the time scale rather than the product type [49], so as we only need to select one type of the IMERG products for error analysis. Additionally, the IMERG-F has been widely used in the hydrological system, so it is regarded as the key issue of this study. The latest hourly, daily, and monthly IMERG Version 06B precipitation estimates from June to August in the summer of 2016–2020, referred to as the IMERG-HF, IMERG-DF, and IMERG-MF, can be obtained by accumulating the IMERG half-hourly estimates in one hour, day and month. All the IMERG estimates used in this research can be downloaded from the Precipitation Measurement Missions website.[1]

C. Ground Reference Data

A gridded gauge data with high spatial ($0.1^\circ \times 0.1^\circ$) and temporal (hourly) resolutions, namely the China Merged Precipitation Analysis (hereafter called CMPA) V1.0 product, is selected as the benchmark. This data is developed by the National Meteorology Information Center of the China Meteorological Administration (CMA) and is publicly available on the official website of the CMA.[2] The CMPA is generated by merging the hourly rain gauge observations from $>$ 30 000 automatic weather stations (AWSs) over Mainland China and CMORPH satellite precipitation estimates using the Probability Density Function-Optimal Interpolation method [50]. Besides, rigorous quality control has been carried out on CMPA, including the extreme values check, internal and spatial consistency check, and is provided in Universal Coordinated Time. More details on the CMPA are described in Shen *et al.* [50]. Over the Sichuan Basin, there are more than 4000 regional-level AWSs and 120 national-level AWSs (see Fig. 1). Compared to the regional-level AWS, the national-level AWS observes more meteorological elements and has more rain gauges (3 versus 1, type SL3-1) for precipitation measure at the same time.

The CMPA is often selected as the benchmark to evaluate the IMERG precipitation estimates [13], [51]–[53]. However, there is an unexpected precipitation bias due to the wind-induced undercatch [42], [54]. The undercatch bias main occurs in the rain gauge measurements. In order to reduce this error, a necessary bias adjustment of gauge-based precipitation observations should be introduced. In this study, we applied the adjustment scheme and some conclusions of Ma *et al.* [54] and Tang *et al.* [42] to correct the ground reference data. More details on adjustment methods are described in their papers [42], [54]. In addition, it is noted that the IMERG-F product uses the gauge data from 4 International Exchange Stations (IES) over the Sichuan Basin, while the data from $>$ 4000 gauge stations (include 4 IES) are used in the CMPA, suggesting that the generation of the CMPA is based on more than 99.9% independent gauge stations. Therefore, we can reasonably believe that the IMERG-F has strong independence with the CMPA and treat the CMPA as reference data.

III. Error Models and Data Preprocessing

A. Error Models

For the additive error model, it is defined as follows:

$$Y_{i,j} = a + b \times X_{i,j} + \varepsilon_{i,j} \tag{1}$$

[1]Online. [Available]: https://disc.gsfc.nasa.gov/datasets/GPM

[2]Online. [Available]: http://data.cma.cn

Where i and j are the indices of the datum. For the gridded data, i and j are the identifiers of grid site sequence and time series, respectively; $Y_{i,j}$ presents a satellite precipitation estimation, referring to the IMERG estimates; $X_{i,j}$ is a gauge measurement, indicating the "truth" reference value of CMPA data; and $\varepsilon_{i,j}$ presents the bias-corrected random error, which has mean 0 and standard deviation σ. In addition, in regression analysis, $\varepsilon_{i,j}$ represents the difference between the reference value and the value predicted by the regression equation. When σ is close to a constant, $\varepsilon_{i,j}$ has homoscedasticity. Conversely, $\varepsilon_{i,j}$ has heteroscedasticity. a and b jointly specify the systematic errors, where a denotes the offset and b is a scale parameter to represent the differences in the dynamic ranges between $Y_{i,j}$ and $X_{i,j}$.

For the multiplicative model, it is defined as follows:

$$Y_{i,j} = a \times X_{i,j}^{b} \times e^{\varepsilon_{i,j}}. \tag{2}$$

Comparing with the additive error model, the relationship between the systematic error (defined by a and b) and $X_{i,j}$ is nonlinear. Besides, the random error $e^{\varepsilon_{i,j}}$ is a nonlinear multiplicative factor, not an addition factor, where the mean and variance of $\varepsilon_{i,j}$ are 0 and σ^2 , respectively.

Based on the central limit theorem, it is a reasonable assumption that the random errors follow a normal distribution pattern. Besides, for a given mean and variance, the entropy of a normal distribution is the highest than that of all other distributions, indicating that a normal distribution for the random errors is highly desirable from a well-behaved error model [27], [55]

$$\varepsilon_{i,j} \sim N\left(0, \sigma^2\right). \tag{3}$$

The additive and multiplicative error models are defined by the parameters a, b, and $\varepsilon_{i,j}$, and the additive model is a 1-D linear regression equation. Therefore, under the assumptions that each residual (random error) is unrelated and the residuals are uncorrelated to the reference data, the three parameters can be estimated easily by using the ordinary least square (OLS) method. The specific calculation is shown in (4) and (5), where *n* is the length of the sequence

$$b = \frac{\sum\left(X_{i,j} - \frac{\sum X_{i,j}}{n}\right) \cdot \left(Y_{i,j} - \frac{\sum Y_{i,j}}{n}\right)}{\sum\left(X_{i,j} - \frac{\sum X_{i,j}}{n}\right)^2} \tag{4}$$

$$a = \frac{\sum Y_{i,j}}{n} - b \times \frac{\sum X_{i,j}}{n}. \tag{5}$$

For the multiplicative error model, we can take the natural logarithm transformation in (2), and the multiplicative model will be converted into the following form:

$$\ln\left(Y_{i,j}\right) = \ln\left(a\right) + b \times \ln\left(X_{i,j}\right) + \varepsilon_{i,j}. \tag{6}$$

Obviously, the transformed multiplicative error model becomes a simple 1-D linear regression similar to the additive error model, and the three parameters can also be obtained by the OLS method.

In addition, the standardized residual (SR) is commonly used to evaluate the fitting effect of the error model [27], [56]. The specific expression is shown in (7). The smaller SR means the better fitting degree and higher accuracy of the error model. The smaller standard deviations of the random errors (or "the standard deviations of the residuals" in the case of OLS) represent that the error model has a better capability to separate systematic and random errors

$$\mathrm{SR} = \sqrt{\frac{1}{n}\sum\left(\varepsilon_{i,j} - \frac{\sum \varepsilon_{i,j}}{n}\right)^2}. \tag{7}$$

Generally, the systematic errors have the characteristics of stability and certainty, while the random errors are minimum and uncertain. In other words, a good error model should be able to separate the systematic and random errors as effectively as possible. The gauge observations and satellite precipitation estimates are obtained based on the precipitation process of the rainy seasons in Sichuan Basin from June to August during the period 2016–2020. We use the observations in the previous four years to evaluate the additive and multiplicative error models at the regional and gridded scales, and use the observations in the last year to validate the predictive capability of the two error models.

B. Data Preprocessing

The data preprocessing includes the following steps.

1) Check the continuity of the IMERG estimates and the CMPA data in temporal and spatial distribution, and then set the abnormal and missing data to the null value.
2) Adjust the time inconsistency of rain gauge data. For instance, the observation at 00:00 actually represents the precipitation from 23:00 to 00:00 of the previous day.
3) Set the threshold of hourly precipitation events occurrence as 0.1 mm/h, and screen out the "joint hit" precipitation events, which include only intensities not less than 0.1 mm/h, are correctly detected by both satellite and gauge at the same time. Because very light precipitation events are not statistically reliable, being more susceptible to noise and artifacts [40], [57], [58].
4) Accumulate hourly "joint hit" data into daily and monthly datasets.

We believe the accumulation of the hourly precipitation errors caused by noise or artifacts may have a negative effect on error modeling.

IV. Results

A. Model's Separative Capability

1) Regional Scale Evaluation: The hourly, daily, and monthly IMERG precipitation estimates have been fitted by the additive and multiplicative models respectively. The results are shown in Fig. 2. For the IMERG-HF and DF, the fitting curves of their additive models do not fit well in the low and medium intensity ranges (< 2 mm/h or < 16 mm/d). In contrast, the multiplicative model performs better in abovementioned ranges. Meanwhile, for the IMERG-MF, the fitting curves of both models match quite well, especially in the medium and high ranges. There are only some differences in positions at the low end (< 25 mm/month). In terms of the three IMERG estimates, the additive model has a better capture capability than that of the

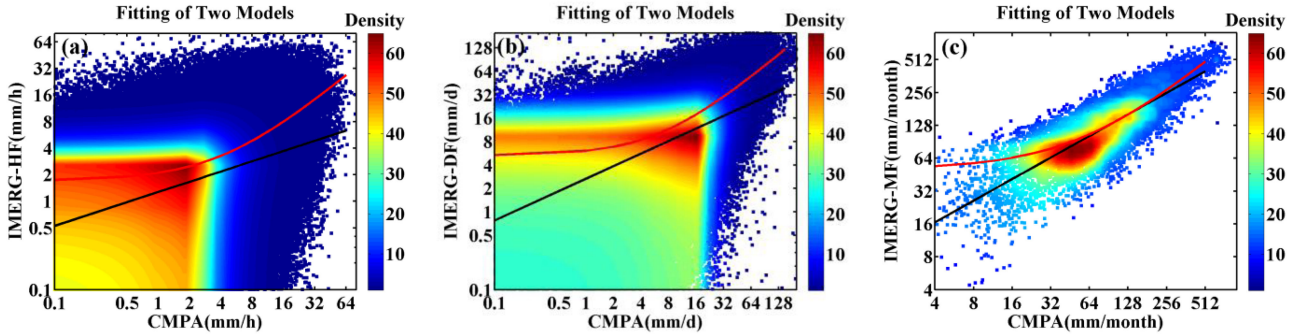

Fig. 2. Scatterplots with density of precipitation and two different fitting curves for (a) the IMERG-HF, (b) IMERG-DF, and (c) IMERG-MF. The red and black lines are the fitting curves of the additive and multiplicative models, respectively. The log–log scales are used in this figure.

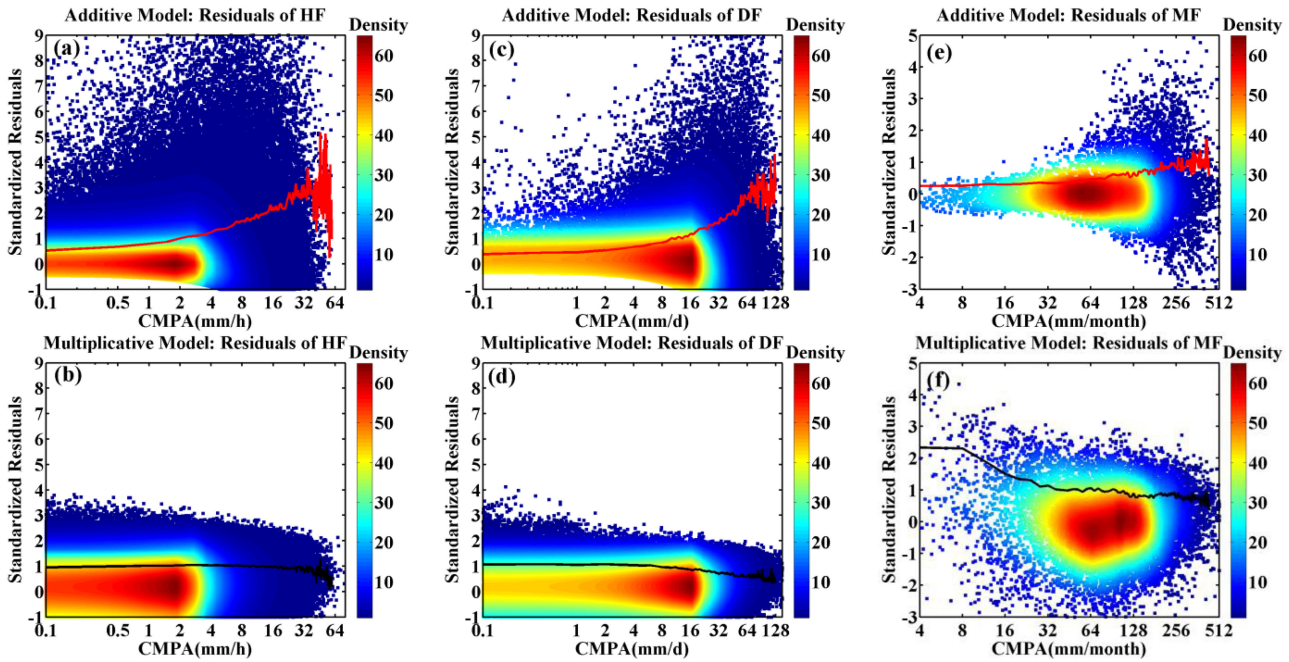

Fig. 3. Comparison of the standardized residuals for the additive and multiplicative models: (a), (c), and (e) represent the additive model's standardized residuals for the IMERG-HF, DF, and MF, respectively. (b), (d), and (f) represent the multiplicative model's standardized residuals for the IMERG-HF, DF, and MF, respectively. The red and black curves are the corresponding model's standard deviations of the residuals within the given precipitation intensity range. The residuals are normalized by their standard deviation. The logarithmic scale is used only on the *X*-axis of this figure.

multiplicative model in some clustering at the high end. Overall, the multiplicative model fits the whole range of the data much better than the additive model in the most range of the hourly and daily IMERG estimates, and there is a similar fitting trend of the both models in the majority of the monthly precipitation.

In order to evaluate model's separative capability, the standard residuals (SRs) of the two models and their corresponding standard deviations of the standard residuals (hereafter called SDSRs) are calculated and plotted in Fig. 3. For the IMERG-HF and DF, the SRs of the additive error model [see Fig. 3(a)] exhibit a systematic increase in scattering with increasing precipitation intensities, while the SRs of the multiplicative model [see Fig. 3(c)] show a more uniform distribution. The SDSRs curves of the additive model [red curves in Fig. 3(a) and (c)] show a gradual upward trend in the ranges of low and medium intensities. The steep slope and amplitude of the fluctuation increases with the increasing precipitation intensity, especially in the condition of high intensity ($>$ 20 mm/h or 48 mm/d). As for the SDSRs of the two models [black curves in Fig. 3(b) and (d)], the two curves are in a constant range for most precipitation intensity. However, when the intensity exceeds 32 mm/h or 64 mm/d, the black curves have a slight variation on the amplitude. And its vibration amplitude is much smaller than that of the red curves. The slight drop at the very high end may be related to the data clustering caused by the saturation of the satellite precipitation estimates under heavy precipitation. In short, the random errors produced from the additive model perform the heteroscedasticity, which suggests that some systematic errors are not separated and "leaked" into the random errors, thus proving the model underfits [27].

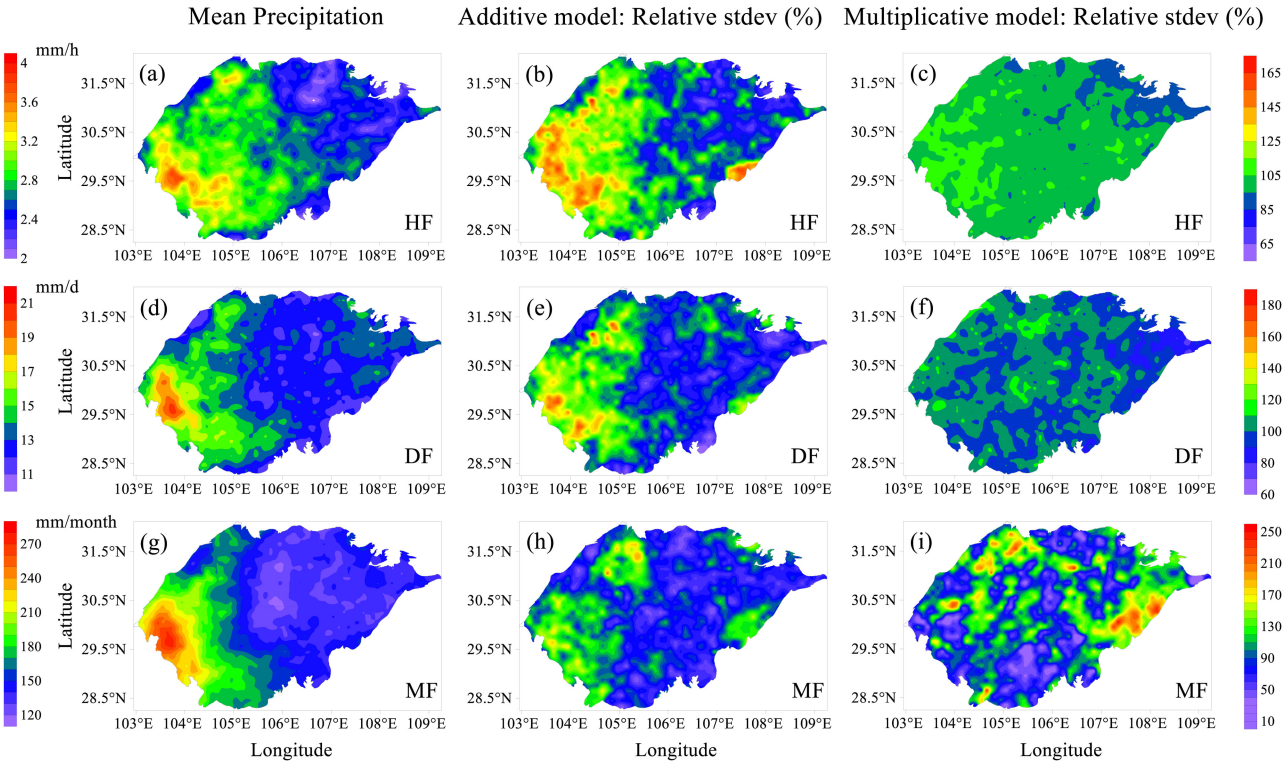

Fig. 4. Spatial distributions of the average rainfall, and the relative standard deviation of the random errors between the additive and multiplicative error models for the IMERG-HF (a)–(c), DF (d)–(f), and MF (g)–(i). The relative value is the ratio of the value to its average.

As for the IMERG-MF, the SDSRs of the additive model [see Fig. 3(e)] remain fairly constant under the intensity less than 256 mm/month and perform a slow upward slope at the high end. However, the SDSRs of the multiplicative model [see Fig. 3(f)] show a sharp downward trend in the low range but exhibit a fairly narrow range of variation in the heavy precipitation (>64 mm/month). Meanwhile, it is noted that the maximum variation of the SDSRs for the additive model is obviously smaller than that of the multiplication model (1.1 versus 1.7) in the whole range of precipitation. In addition, the additive model's SDSRs obtained by monthly precipitation present significantly smaller fluctuation amplitudes than that of the hourly and daily precipitation under heavy precipitation. With regards to the overall performance of the two models, the additive model is more suitable for the error analysis of the low and medium monthly precipitation, while the multiplicative model may prevail in the error analysis of heavy precipitation.

2) Grid-Scale Evaluation: According to the spatial distributions of SDSRs shown in Fig. 4, the SDSRs of the IMER-HF and DF for the additive model present high values in heavy precipitation regions, such as the southwest and southeast [see Fig. 4(b) and (e)]. This suggests that the random errors of the additive error model maintain good correlation among the spatial distributions of the average rainfall [see Fig. 4(a) and (d)]. However, the random errors in the multiplicative model [see Fig. 4(c) and (f)] exhibit relatively consistent values in the entire spatial range of the basin, which means random errors of the multiplicative model are almost independent of the spatial distributions of the average rainfall. As for the IMERG-MF, in comparison, the random errors of the additive model show more uniform and less correlation with the average precipitation than of the multiplicative model in most regions, except in the southwest part of the basin.

The above analysis results on regional and gridded scales show that for the hourly and daily IMERG precipitation estimates, the random errors of the additive model have heteroscedasticity. This is because the additive model (in hourly and daily estimates) violates the assumption of the normal distribution of the random errors when using the OLS method to estimate model parameters. In addition, when the precipitation intensity exceeds 4 mm/h or 16 mm/d, the additive model shows some unstable random errors, which implies that the random errors are mixed with the systematic errors. Conversely, the random errors of the multiplicative model show homoscedasticity. This suggests that the multiplicative model has a better capability to distinguish the systematic errors from the random errors, and has better fitting than that of the additive error model. As for the IMERG monthly estimates, the additive error model is a relatively better choice considering by comparing the overall performance of both models. However, it's separative capability decrease slightly for heavy precipitation.

B. Model's Predictive Capability

The parameters of the additive and multiplicative models are determined by the IMERG and CMPA datasets from 2016 to 2019 (the first four years).

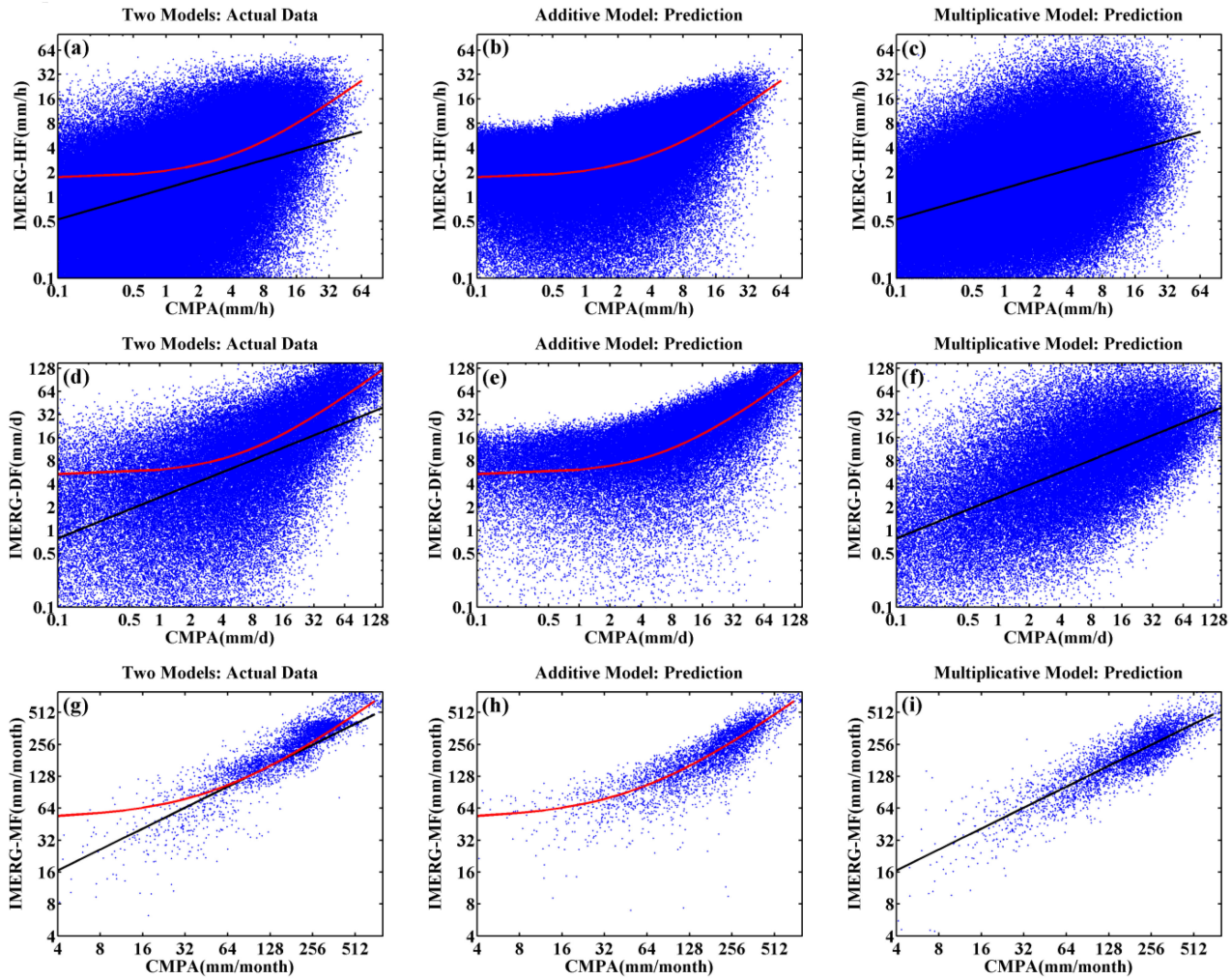

Fig. 5. Scatterplots of the actual and predicted data for the IMERG-HF (a)–(c), DF (d)–(f), MF (g)–(i) estimates for the summer of 2020: (a), (d), and (g) are the actual scatterplots; (b), (e), (h) and (c), (f), (i) are the prediction for the additive and multiplicative models, respectively. The red and black lines are the regression lines of the historical calibration data for the additive and multiplicative models, respectively.

The predictive capability of errors is the key to evaluating the model's performance. Therefore, we use the ground reference data for the summer of 2020 and then establish the error model to predict the hourly, daily, and monthly IMERG precipitation estimates. The scatterplots of the actual gauge versus satellite predicted data for the summer of 2020 are shown in Fig. 5.

Judging from the similarity of the scatterplots between the predicted and the actual data, the predictions of the additive model for the hourly and daily IMERG estimates [see Fig. 5(b) and (e)] show an overconcentrated clustering characteristic in the whole intensity range, especially under high precipitation intensity. This implies that the predictions cannot reproduce the scatter points distribution of the actual data well. Conversely, the predictions of the multiplicative model [see Fig. 5(c) and (f)] are found to coincide with the actual data [see Fig. 5(a) and (d)]. As for the monthly IMERG estimates, both of the error models successfully predicted the clustering characteristics in the medium and high intensity range [see Fig. 5(g), (h), and (i)]. However, for the IMERG-MF, these data points can be better captured by the additive model than that of the multiplicative model when taking the scatterplots of the actual data as the standard reference, especially at the low end (< 32 mm/month).

To further evaluate the predictive capability of the two models, we analyze the statistics on the probability density functions (PDFs) and precipitation accumulation with different intensities and calculate the correlation coefficient (CC) between the predicted and actual data. The relevant results are shown in Fig. 6.

As for the hourly and daily IMERG estimates, the comparison of the two models' predicted PDFs shows that the amplitude variation of the magenta and black curves [see Fig. 6(b) and (f)] is highly consistent, while the red and black curves [see Fig. 6(a) and (e)] have a noticeable gap in the low intensity ranges. The CC values of the multiplicative model are obviously higher than those of the additive model. As shown in Fig. 6(c), (d), (g), and (h), for the precipitation accumulation, the additive and multiplicative models have the similar predictive capability, but the performance of the latter is still slightly better than that of the former. Moreover, for the monthly IMERG precipitation estimate, the CC values of the predicted PDFs for the two models are very close (the difference is 0.06). However, the two

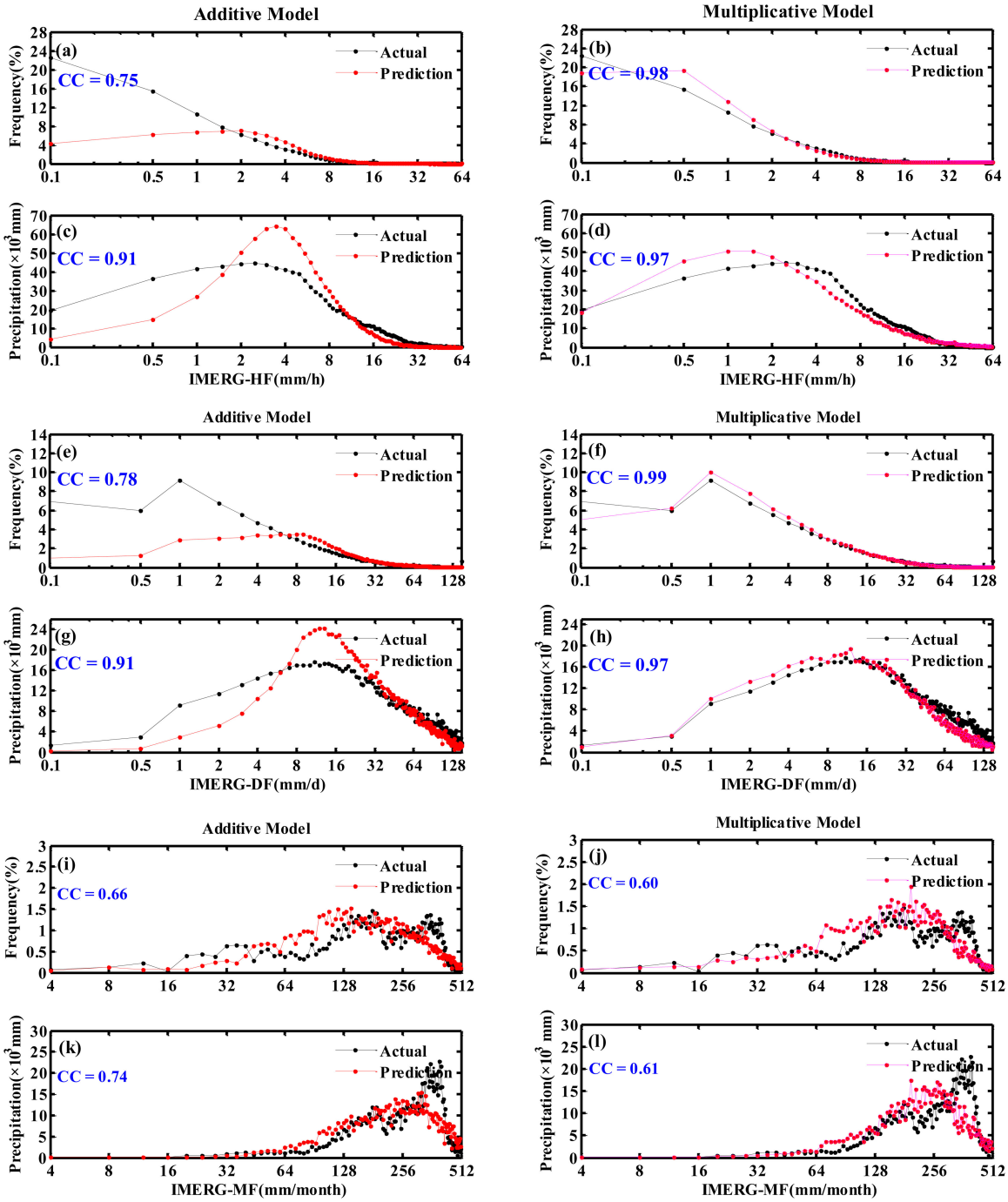

Fig. 6. Comparison of the additive (left) and multiplicative (right) error models' predictive capability for the IMERG-HF, DF, and MF estimates [(a)–(d), (e)–(h), (i)–(l)]. Metrics include the PDFs and cumulative precipitation of various intensities. Correlation coefficients (CC) between actual and predicted data are labeled.

models show a clear difference in the prediction of precipitation accumulation (the difference is 0.13). It is also worth mentioning that predictive capability of both models performs poorly with the heavy precipitation (>340 mm/month).

In conclusion, for the hourly and daily IMERG precipitation estimates, whether the PDFs or precipitation accumulation with different intensities, the multiplicative model has a better capability to reproduce the error characteristics than the additive model. However, for the monthly IMERG precipitation estimates, the additive model shows a relatively better predictive capability than the multiplicative model for most intensities of precipitation, except for the heavy precipitation.

V. Discussion

For the hourly and daily IMERG precipitation estimates, the random errors that separated by using the additive model have obvious heteroscedasticity, which suggests that some systematic errors are not separated well and "leaked" into the random errors. Namely, the random errors increase rapidly with the increasing

precipitation intensities. In contrast, the random errors in the multiplicative model show a more uniform distribution and exhibit homoscedasticity. The phenomenon of "leaked" can also be found from the comparison of the spatial distribution of the random errors and mean precipitation. Furthermore, the multiplicative model can reproduce the error characteristics of the actual data better than that of the additive model. This can be explained by the definition of the additive model. The logical explanation is systematic errors specified by parameters a and b are a linear function of the reference data, while many existing studies have indicated otherwise [23], [27]. Thus, the additive model may not completely capture the systematic errors. Conversely, as for the monthly IMERG precipitation estimates, the additive model has a better separative and predictive capabilities for most intensities of precipitation than the multiplicative model, except for the heavy precipitation. The reasonable explanation for this result is that the details of the errors in satellite precipitation measurements are gradually smoothed out with the decrease of temporal and spatial resolutions, in other words, the magnitude of precipitation variability is much suppressed, so that both precipitation and its errors are closer to the normal distribution [29], [59], then the additive model may prevail. Moreover, Tian *et al*. believe that as the temporal resolution increases (daily or finer), the probability distributions and errors of precipitation are closer to the Gamma or lognormal distribution [27], that makes the multiplicative model a better choice. Then, they speculated that the additive model may prevail for the precipitation with some coarser temporal resolutions. Our conclusions in this article confirmed the speculations of Tian *et al.*

Although the multiplicative or additive model is simple and easy to implement, the two models cannot perfectly explain and accurately quantify the errors. Nevertheless, more complex error models can certainly be developed, but it should be noted that the complex model may bring greater challenges to the calibration improvement of measuring instruments and optimization of precipitation estimation algorithms. In view of the simplicity, the practicability, and the capabilities of the error separation and prediction in the error model designing, we believe that the additive and multiplicative models have certain advantages in separating the systematic and random errors and predicting the errors for the satellite precipitation at the corresponding temporal resolution.

It is noted that both CMPA and IMERG contain the CMORPH information to a certain extent. Thus, the bias of CMORPH may increase the errors of the CMPA and the IMERG. To resolve this problem, the CMPA developers have adopted the PDF method to correct the systematic bias of CMORPH [50]. Accordingly, the improved method used in CMPA could achieve more gauge observations by increasing the weighting in the areas where the gauge measurements are available, while retaining CMORPH information in the areas that lacking of gauges. Since the Sichuan Basin own high-density ground gauge networks, data from ground gauge plays an absolutely leading role in the generation of the CMPA in this area [45], [50]. In fact, CMPA's high accuracy has been demonstrated by the CMPA developers and users using the ground gauge data as a reference in different terrains of China [50], [60].

We treated the gauge reference data as error free when evaluating the suitability of the two models, which is not absolutely true (even though a necessary bias adjustment of gauge-based observations has been applied to correct the undercatch bias). This is because the errors of the CMPA data come from many sources, such as wind-induced undercatch, wet/evaporation loss, and merging methods. However, in practice, Tian *et al*. [27] concluded that the errors in the gauge-based observations are much smaller than those in the satellite-based estimates. Even so, we still have to admit that the independence of CMPA may be a potential factor affecting the error model's fitting. But we believe that neither the assumption of no free nor the independence of data should not change the nature of our conclusions in this study. Furthermore, a reasonable assumption is that the errors of satellite-based precipitation are only functions of the reference rain rate and are not designed to analyze the errors from spatial patterns [27]. Thus, the model established in this study is more suitable for gridded and regional precipitation studies. The errors caused by other geophysical parameters, such as topography, will be indirectly reflected in the modeling parameters.

This study focuses on the "joint hit" precipitation events, only the intensities not less than 0.1 mm/h in both IMERG estimates and CMPA data are used in the model designed (hereafter, referred as to Strategy-1). Because we recognized that the precipitation with lower intensities in either the gauge data or the satellite estimates are statistically unreliable, being more susceptible to noise and artifacts [40], [57], [58]. It should be noted that another strategy is similar to Roebeling *et al*. [61] and Li *et al.* [62], which considers the zero precipitation (hereafter, referred as to Strategy-2). In fact, both Strategy-1 and Strategy-2 can be used to analyze the error characteristics of satellite precipitation estimates, but the former analyses the errors of hit precipitation, while the latter analyses the errors of total precipitation events. In particular, Strategy-1 allows to concentrate on precipitation rates where the skill of the satellite algorithm is more impacting [42]. In addition, because the "missed precipitation" and "false precipitation" events that take zero precipitation into consideration are the important contributors to the total errors, they should be modeled as separate error components in our follow-up research.

VI. Conclusion

The additive and multiplicative models have been widely used to quantify the errors of precipitation measurements, but the error characteristics of the two models may be significantly different for the same set of precipitation data due to their different definitions of errors. To evaluate which error model can better quantify or simulate the errors of the IMERG precipitation estimates, we have comprehensively analyzed and compared the error characteristics of the additive and multiplicative models for the hourly, daily, and monthly IMERG precipitation estimates over the Sichuan Basin during the summer from 2016 to 2020. Two criteria, model's the separative capability of the systematic errors and predictive capability of the future precipitation, are employed to evaluate the applicability of each model. Our main conclusions are summarized as follows.

1) For the hourly and daily IMERG precipitation estimates, the multiplicative error model is preferable to the additive model in estimating the model's separative and predictive capabilities. It can capture the systematic errors more completely and make the random errors remain in a fairly constant range. Besides, the multiplicative model outperforms the additive model in predicting the precipitation events and the error characteristics.
2) Regarding the monthly IMERG precipitation estimates, the additive error model is a better choice by comparing the overall performance of both models. It should be pointed out that the additive model has obviously higher separative and predictive capabilities for the low and medium precipitation (<256 mm/month) than the multiplicative model. However, at the high end, both models have some weakness, such as the heteroscedasticity of random errors due to poor separative capability, and strong underestimation due to reduced predictive capability. So, the additive model should be used with caution when quantifying the errors of heavy monthly precipitation.

REFERENCES

[1] M. Bollasina, Y. Ming, and V. Ramaswamy, "Anthropogenic aerosols and the weakening of the south Asian summer monsoon," *Science,* vol. 334, no. 6055, pp. 502–505, 2011, doi: 10.1126/science.1204994.

[2] C. Kidd *et al.*, "Intercomparison of high-resolution precipitation products over northwest Europe," *J. Hydrometeorol.,* vol. 13, no. 1, pp. 67–83, 2012.

[3] R. Hadji, A. E. Boumazbeur, Y. Limani, M. Baghem, A. E. M. Chouabi, and A. Demdoum, "Geologic, topographic and climatic controls in landslide hazard assessment using GIS modeling: A case study of Souk Ahras region, NE Algeria," *Quaternary Int.,* vol. 302, pp. 224–237, 2013, doi: 10.1016/j.quaint.2012.11.027.

[4] H. Vergara *et al.*, "Effects of resolution of satellite-based rainfall estimates on hydrologic modeling skill at different scales," *J. Hydrometeorol.,* vol. 15, no. 2, pp. 593–613, 2014.

[5] A. Y. Hou *et al.*, "The global precipitation measurement mission," *Bull. Amer. Meteorological Soc.,* vol. 95, no. 5, pp. 701–722, 2014.

[6] Z. Zhaozhao, C. Haonan, S. Qian, and L. Jun, "Spatial downscaling of IMERG considering vegetation index based on adaptive lag phase," *IEEE Trans. Geosci. Remote Sens.*, to be published, doi: 10.1109/TGRS.2021.3070417.

[7] G. Tang, Y. Ma, D. Long, L. Zhong, and Y. Hong, "Evaluation of GPM day-1 IMERG and TMPA version-7 legacy products over Mainland China at multiple spatiotemporal scales," *J. Hydrol.,* vol. 533, pp. 152–167, 2016, doi: 10.1016/j.jhydrol.2015.12.008.

[8] G. J. Huffman *et al.*, "The TRMM multisatellite precipitation analysis (TMPA): Quasi-global, multiyear, combined-sensor precipitation estimates at fine scales," *J. Hydrometeorol.,* vol. 8, no. 1, pp. 38–55, 2007, doi: 10.1175/JHM560.1.

[9] G. J. Huffman *et al.*, "NASA global precipitation measurement (GPM) integrated multi-satellite retrievals for GPM (IMERG) algorithm theoretical basis document (ATBD) version 06," 2020. Accessed: Jun. 23, 2020. [Online]. Available: https://pmm.nasa.gov/sites/default/files/document_files/IMERG_ATBD_V06.pdf

[10] Z. Liu, "Comparison of integrated multisatellite retrievals for GPM (IMERG) and TRMM multisatellite precipitation analysis (TMPA) monthly precipitation products: Initial results," *J. Hydrometeorol.,* vol. 17, no. 3, pp. 777–790, 2016, doi: 10.1175/JHM-D-15-0068.1.

[11] G. Tang *et al.*, "Statistical and hydrological comparisons between TRMM and GPM level-3 products over a midlatitude basin: Is day-1 IMERG a good successor for TMPA 3B42V7?," *J. Hydrometeorol.,* vol. 17, no. 1, pp. 121–137, 2016, doi: 10.1175/JHM-D-15-0059.1.

[12] K. Kim, J. Park, J. Baik, and M. Choi, "Evaluation of topographical and seasonal feature using GPM IMERG and TRMM 3B42 over far-east Asia," *Atmospheric Res.,* vol. 187, pp. 95–105, 2017, doi: 10.1016/j.atmosres.2016.12.007.

[13] Z. Wang, R. Zhong, C. Lai, and J. Chen, "Evaluation of the GPM IMERG satellite-based precipitation products and the hydrological utility," *Atmospheric Res.,* vol. 196, pp. 151–163, 2017, doi: 10.1016/j.atmosres.2017.06.020.

[14] X. Lu, M. Wei, G. Tang, and Y. Zhang, "Evaluation and correction of the TRMM 3B43V7 and GPM 3IMERGM satellite precipitation products by use of ground-based data over Xinjiang, China," *Environ. Earth Sci.,* vol. 77, no. 5, 2018, Art. no. 209, doi: 10.1007/s12665-018-7378-6.

[15] F. Xu *et al.*, "Systematical evaluation of GPM IMERG and TRMM 3B42V7 precipitation products in the Huang-Huai-Hai plain, China," *Remote Sens.,* vol. 11, no. 6, 2019, Art. no. 697, doi: 10.3390/rs11060697.

[16] C. M. Naud, J. F. Booth, M. Lebsock, and M. Grecu, "Observational constraint for precipitation in extratropical cyclones: Sensitivity to data sources," *J. Appl. Meteorol. Climatol.,* vol. 57, no. 4, pp. 991–1009, 2018, doi: 10.1175/JAMC-D-17-0289.1.

[17] C. Huang *et al.*, "How well can IMERG products capture typhoon extreme precipitation events over southern China," *Remote Sens.,* vol. 11, no. 1, 2019, Art. no. 70, doi: 10.3390/rs11010070.

[18] P. Mazzoglio, F. Laio, S. Balbo, P. Boccardo, and F. Disabato, "Improving an extreme rainfall detection system with GPM IMERG data," *Remote Sens.,* vol. 11, no. 6, 2019, Art. no. 677, doi: 10.3390/rs11060677.

[19] C. M. Naud, J. Jeyaratnam, J. F. Booth, M. Zhao, and A. Gettelman, "Evaluation of modeled precipitation in oceanic extratropical cyclones using IMERG," *J. Climate,* vol. 33, no. 1, pp. 95–113, 2020, doi: 10.1175/JCLI-D-19-0369.1.

[20] S. Tang, R. Li, J. He, H. Wang, X. Fan, and S. Yao, "Comparative evaluation of the GPM IMERG early, late, and final hourly precipitation products using the CMPA data over Sichuan basin of China," *Water,* vol. 12, no. 2, 2020, Art. no. 554, doi: 10.3390/w12020554.

[21] S. Tang, R. Li, J. He, X. Fan, H. Wang, and S. Yao, "Seasonal error component analysis of the GPM IMERG version 05 precipitation estimations over Sichuan basin of China," *Earth Space Sci.,* vol. 8, no. 1, 2020, Art. no. e2020EA001259, doi: 10.1029/2020EA001259.

[22] A. Aghakouchak, A. Bardossy, and E. Habib, "Copula-based uncertainty modelling: Application to multisensor precipitation estimates," *Hydrological Processes,* vol. 24, no. 15, pp. 2111–2124, 2010, doi: 10.1002/hyp.7632.

[23] M. Gebremichael, G. Y. Liao, and J. Yan, "Nonparametric error model for a high resolution satellite rainfall product," *Water Resour. Res.,* vol. 47, no. 7, p. W07504, 2011, doi: 10.1029/2010WR009667.

[24] J. Yan and M. Gebremichael, "Estimating actual rainfall from satellite rainfall products," *Atmospheric Res.,* vol. 92, no. 4, pp. 481–488, 2009, doi: 10.1016/j.atmosres.2009.02.004.

[25] V. Maggioni, M. R. P. Sapiano, R. F. Adler, Y. Tian, and G. J. Huffman, "An error model for uncertainty quantification in high-time-resolution precipitation products," *J. Hydrometeorol.,* vol. 15, no. 3, pp. 1274–1292, 2014, doi: 10.1175/JHM-D-13-0112.1.

[26] D. B. Wright, D. B. Kirschbaum, and S. Yatheendradas, "Satellite precipitation characterization, error modeling, and error correction using censored shifted gamma distributions," *J. Hydrometeorol.,* vol. 18, no. 10, pp. 2801–2815, 2017, doi: 10.1175/JHM-D-17-0060.1.

[27] Y. Tian *et al.*, "Modeling errors in daily precipitation measurements: Additive or multiplicative?," *Geophys. Res. Lett.,* vol. 40, no. 10, pp. 2060–2065, 2013, doi: 10.1002/grl.50320.

[28] W. G. Lawson and J. A. Hansen, "Alignment error models and ensemble-based data assimilation," *Monthly Weather Rev.,* vol. 133, no. 6, pp. 1687–1709, 2005.

[29] S. Sorooshian, K. Hsu, X. Gao, H. V. Gupta, B. Imam, and D. Braithwaite, "Evaluation of PERSIANN system satellite-based estimates of tropical rainfall," *Bull. Amer. Meteorological Soc.,* vol. 81, no. 9, pp. 2035–2046, 2000.

[30] R. Joyce, J. E. Janowiak, P. A. Arkin, and P. Xie, "CMORPH: A method that produces global precipitation estimates from passive microwave and infrared data at high spatial and temporal resolution," *J. Hydrometeorol.,* vol. 5, no. 3, pp. 487–503, 2004.

[31] T. Kubota *et al.*, "Global precipitation map using satellite-borne microwave radiometers by the GSMaP project: Production and validation," *IEEE Trans. Geosci. Remote Sens.,* vol. 45, no. 7, pp. 2259–2275, Jul. 2007.

[32] C. J. Willmott, "On the validation of models," *Phys. Geography,* vol. 2, no. 2, pp. 184–194, 1981, doi: 10.1080/02723646.1981.10642213.

[33] E. Habib, A. Henschke, and R. F. Adler, "Evaluation of TMPA satellite-based research and real-time rainfall estimates during six tropical-related heavy rainfall events over Louisiana, USA," *Atmospheric Res.,* vol. 94, no. 3, pp. 373–388, 2009, doi: 10.1016/j.atmosres.2009.06.015.

[34] R. Roca, P. Chambon, I. Jobard, P. Kirstetter, M. Gosset, and J. C. Berges, "Comparing satellite and surface rainfall products over west africa at meteorologically relevant scales during the AMMA campaign using error estimates," *J. Appl. Meteorol. Climatol.,* vol. 49, no. 4, pp. 715–731, 2010, doi: 10.1175/2009JAMC2318.1.
[35] A. Aghakouchak, A. Mehran, H. Norouzi, and A. Behrangi, "Systematic and random error components in satellite precipitation data sets," *Geophys. Res. Lett.,* vol. 39, no. 9, p. L09406, 2012, doi: 10.1029/2012GL051592.
[36] J. C. Berges, I. Jobard, F. Chopin, and R. Roca, "EPSAT-SG: A satellite method for precipitation estimation; its concepts and implementation for the AMMA experiment," *Annales Geophysicae,* vol. 28, no. 1, pp. 289–308, 2010.
[37] F. Hossain and E. N. Anagnostou, "A two-dimensional satellite rainfall error model," *IEEE Trans. Geosci. Remote Sens.,* vol. 44, no. 6, pp. 1511–1522, Jun. 2006.
[38] G. J. Ciach, W. F. Krajewski, and G. Villarini, "Product-error-driven uncertainty model for probabilistic quantitative precipitation estimation with NEXRAD data," *J. Hydrometeorol.,* vol. 8, no. 6, pp. 1325–1347, 2007, doi: 10.1175/2007JHM814.1.
[39] G. Villarini, W. F. Krajewski, G. J. Ciach, and D. L. Zimmerman, "Product-error-driven generator of probable rainfall conditioned on WSR-88D precipitation estimates," *Water Resour. Res.,* vol. 45, no. 1, p. W01404, 2009, doi: 10.1029/2008WR006946.
[40] J. Tan, W. A. Petersen, and A. Tokay, "A novel approach to identify sources of errors in IMERG for GPM ground validation," *J. Hydrometeorol.,* vol. 17, no. 9, pp. 2477–2491, 2016, doi: 10.1175/JHM-D-16-0079.1.
[41] S. Alemohammad, K. McColl, A. Konings, D. Entekhabi, and A. Stoffelen, "Characterization of precipitation product errors across the United States using multiplicative triple collocation," *Hydrol. Earth System Sci.,* vol. 19, no. 8, pp. 3489–3503, 2015, doi: 10.5194/hess-19-3489-2015.
[42] G. Tang, "Characterization of the systematic and random errors in satellite precipitation using the multiplicative error model," *IEEE Trans. Geosci. Remote Sens.,* to be published, doi: 10.1109/TGRS.2020.3028525.
[43] Z. Qiuxue, K. Lan, J. Xingwen, and L. Ying, "Relationship between heavy rainfall and altitude in mountainous areas of Sichuan basin," *Meteorological Monthly,* vol. 045, no. 6, pp. 811–819, 2019, doi: 10.7519/j.issn.1000-0526.2019.06.007.
[44] L. Ping, Y. Rucong, and Z. Tianjun, "Numerical simulation of the midnight rainfall over Sichuan basin during August 2003," *Acta Meteorologica Sinica,* vol. 66, no. 3, pp. 371–380, 2008.
[45] P. F. Shen and Y. C. Zhang, "Numerical simulation of diurnal variation of summer precipitation in Sichuan basin," *Plateau Meteorol.,* vol. 30, no. 4, pp. 860–868, 2011, https://doi.org/1000-0534(2011)04-0860-09.
[46] H. Hu, X. Mao, and L. Liang, "Temporal and spatial variations of extreme precipitation events of flood season over Sichuan basin in last 50 years," *Acta Geographica Sinica,* vol. 64, no. 3, pp. 278–288, 2009, doi: 10.1007/978-1-4020-9623-5_5.
[47] C. Dan, Z. Changyan, X. Guangming, and D. Mengyu, "Characteristics of climate change of summer rainstorm in Sichuan basin in the last 53 years," *Plateau Meteorol.,* vol. 37, no. 1, pp. 197–206, 2018, doi: 10.7522/j.issn.1000-0534.2017.00022.
[48] M. L. Tan and H. Santo, "Comparison of GPM IMERG, TMPA 3B42 and PERSIANN-CDR satellite precipitation products over Malaysia," *Atmospheric Res.,* vol. 202, pp. 63–76, 2018, doi: 10.1016/j.atmosres.2017.11.006.
[49] H. McMillan, B. Jackson, M. Clark, D. Kavetski, and R. Woods, "Rainfall uncertainty in hydrological modelling: An evaluation of multiplicative error models," *J. Hydrol.,* vol. 400, nos. 1/2, pp. 83–94, 2011, doi: 10.1016/j.jhydrol.2011.01.026.
[50] Y. Shen, P. Zhao, Y. Pan, and J. Yu, "A high spatiotemporal gauge-satellite merged precipitation analysis over China," *J. Geophys. Res.,* vol. 119, no. 6, pp. 3063–3075, 2014, doi: 10.1002/2013JD020686.
[51] J. Su, H. Lü, W. T. Crow, Y. Zhu, and Y. Cui, "The effect of spatiotemporal resolution degradation on the accuracy of IMERG products over the Huai river basin," *J. Hydrometeorol.,* vol. 21, no. 5, pp. 1073–1088, 2020, doi: 10.1175/JHM-D-19-0158.1.
[52] J. Su, H. Lu, Y. Zhu, X. Wang, and G. Wei, "Component analysis of errors in four GPM-based precipitation estimations over mainland China," *Remote Sens.,* vol. 10, no. 9, 2018, Art. no. 1420, doi: 10.3390/rs10091420.
[53] S. Zhu, Y. Shen, and Z. Ma, "A new perspective for charactering the spatiotemporal patterns of the error in GPM IMERG over mainland China," *Earth Space Sci.,* vol. 8, no. 1, pp. 1–16, 2021, doi: 10.1029/2020EA001232.
[54] Y. Ma, Y. Zhang, D. Yang, and S. B. Farhan, "Precipitation bias variability versus various gauges under different climatic conditions over the third pole environment (TPE) region," *Int. J. Climatol.,* vol. 35, no. 7, pp. 1201–1211, 2015, doi: 10.1002/joc.4045.
[55] E. T. Jaynes, "Information theory and statistical mechanics," *Phys. Rev.,* vol. 106, no. 2, pp. 620–630, 1957, doi: 10.1103/PhysRev.106.620.
[56] R. Li, J. He, S. Tang, F. Miao, and X. Fan, "Observational consistency comparison and analyses of an X-band solid-state radar and an X-band klystron doppler radar," *J. Atmospheric Ocean. Technol.,* vol. 34, no. 10, pp. 2177–2202, 2017, doi: 10.1175/JTECH-D-16-0220.1.
[57] A. G. Barnston and J. L. Thomas, "Rainfall measurement accuracy in FACE: A comparison of gage and radar rainfalls," *J. Appl. Meteorol.,* vol. 22, no. 12, pp. 2038–2052, 1983.
[58] Y. Tian and C. D. Peterslidard, "Systematic anomalies over inland water bodies in satellite-based precipitation estimates," *Geophys. Res. Lett.,* vol. 34, no. 14, p. L14403, 2007, doi: 10.1029/2007GL030787.
[59] P. D. Sardeshmukh, G. P. Compo, and C. Penland, "Changes of probability associated with El Nino," *J. Climate,* vol. 13, no. 24, pp. 4268–4286, 2000.
[60] L. Shi, Y. Wan, D. Zhang, Q. Wang, and J. Yang, "Precision evaluation of CMPA remote sensing precipitation data in different terrains of China," *J. Meteorological Sci.,* vol. 38, no. 5, pp. 616–624, 2018, doi: 10.3969/2017jms.0059.
[61] R. Roebeling, E. Wolters, J. Meirink, and H. Leijnse, "Triple collocation of summer precipitation retrievals from SEVIRI over Europe with gridded rain gauge and weather radar data," *J. Hydrometeorol.,* vol. 13, no. 5, pp. 1552–1566, 2012, doi: 10.1175/jhm-d-11-089.1.
[62] C. Li, G. Tang, and Y. Hong, "Cross-evaluation of ground-based, multi-satellite and reanalysis precipitation products: Applicability of the triple collocation method across mainland China," *J. Hydrol.,* vol. 562, pp. 71–83, 2018, doi: 10.1016/j.jhydrol.2018.04.039.

Shunxian Tang received the Ph.D. degree in atmospheric physics and atmospheric environment from the Institute of Atmospheric Physics, Chinese Academy of Sciences, Beijing, China, in 2019.

He is currently a Precipitation Retrieval Algorithm Researcher with the Chengdu University of Information Technology, Chengdu, China. His work focuses on the development of software and technologies for processing and generating precipitation products using Earth observation data from several remote-sensing platforms including ground-based weather radar, airborne radar, and various satellite platforms.

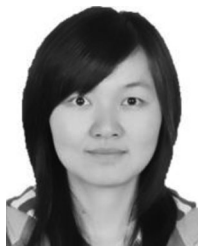

Rui Li received the Ph.D. degree from the College of Geophysics, Chengdu University of Technology, Chengdu, China, in 2019.

She is currently a Weather Radar Algorithm Researcher with the Chengdu University of Information Technology. Her research interests include Weather Radar signal processing, data processing, geophysical retrievals, and the use of remote sensing data for weather forecast, with current focus on the modeling and analysis of precipitation using satellite observations from several remote-sensing platforms.

Jianxin He received the M.Sc. degree from the Chinese Academy of Meteorological Sciences, Beijing, China, in 1990.

He is the Vice President of Chengdu University of Information Technology (CUIT), a Ph.D. Supervisor, and the Director of the Key Laboratory of Atmospheric Sounding (KLAS). He is a Full Professor with CUIT. His main research interests span a broad range of active remote sensing and atmospheric sciences, including radar system construction, digital signal processing, hardware prototype development, precipitation classification and estimation, and weather prediction. He has improved the signal processing methods and data quality control theory of Doppler and dual-polarization weather radars and made great efforts to develop FPGA application in weather radar and has also improved the detection performance and stability of weather radars. The weather radar signal processors developed are widely used in the new generation of weather radar networks, which promotes the wide application and social benefits of weather radar.